



THE UNIVERSITY *of* EDINBURGH

Edinburgh Research Explorer

Structural and Biophysical Studies on Two Promoter Recognition Domains of the Extra-cytoplasmic Function Factor C from *Mycobacterium tuberculosis*

Citation for published version:

Thakur, KG, Joshi, AM & Gopal, B 2007, 'Structural and Biophysical Studies on Two Promoter Recognition Domains of the Extra-cytoplasmic Function Factor C from *Mycobacterium tuberculosis*', *Journal of Biological Chemistry*, vol. 282, no. 7, pp. 4711-4718. <https://doi.org/10.1074/jbc.M606283200>

Digital Object Identifier (DOI):

[10.1074/jbc.M606283200](https://doi.org/10.1074/jbc.M606283200)

Link:

[Link to publication record in Edinburgh Research Explorer](#)

Document Version:

Peer reviewed version

Published In:

Journal of Biological Chemistry

General rights

Copyright for the publications made accessible via the Edinburgh Research Explorer is retained by the author(s) and / or other copyright owners and it is a condition of accessing these publications that users recognise and abide by the legal requirements associated with these rights.

Take down policy

The University of Edinburgh has made every reasonable effort to ensure that Edinburgh Research Explorer content complies with UK legislation. If you believe that the public display of this file breaches copyright please contact openaccess@ed.ac.uk providing details, and we will remove access to the work immediately and investigate your claim.



Published in final edited form as:

J Biol Chem. 2007 February 16; 282(7): 4711–4718.

Structural and biophysical studies on two promoter recognition domains of the extra-cytoplasmic function σ factor σ^C from *Mycobacterium tuberculosis*

Krishan Gopal Thakur, Anagha Madhusudan Joshi, and B. Gopal

Molecular Biophysics Unit, Indian Institute of Science, Bangalore 560 012, India

Summary

σ factors are transcriptional regulatory proteins that bind to the RNA polymerase and dictate gene expression. The extracytoplasmic function σ factors (ECF) govern the environment dependent regulation of transcription. ECF σ factors have two domains σ_2 and σ_4 that recognize the -10 and -35 promoter elements. However, unlike the primary σ factor σ^A , the ECF σ factors lack σ_3 , a region that helps in the recognition of the extended -10 element and $\sigma_{1.1}$, a domain involved in the auto-inhibition of σ^A in the absence of core RNA polymerase. *Mycobacterium tuberculosis* σ^C is an ECF σ factor that is essential for the pathogenesis and virulence of *M. tuberculosis* in the mouse and guinea pig models of infection. However, unlike other ECF σ factors, σ^C does not appear to have a regulatory anti- σ factor located in the same operon. We also note that *Mycobacterium tuberculosis* σ^C differs from the canonical ECF σ factors as it has an N-terminal domain comprising of 126 amino acids that precedes the σ^C_2 and σ^C_4 domains. In an effort to understand the regulatory mechanism of this protein, the crystal structures of the σ^C_2 and σ^C_4 domains of σ^C were determined. These promoter recognition domains are structurally similar to the corresponding domains of σ^A despite the low sequence similarity. Fluorescence experiments using the intrinsic tryptophan residues of σ^C_2 as well as surface plasmon resonance measurements reveal that the σ^C_2 and σ^C_4 domains interact with each other. Mutational analysis suggests that the Pribnow box binding region of σ^C_2 is involved in this inter-domain interaction. Interaction between the promoter recognition domains in *M. tuberculosis* σ^C are thus likely to regulate the activity of this protein even in the absence of an anti- σ factor.

Introduction

The slow growing pathogen, *Mycobacterium tuberculosis*, has only one ribosomal RNA operon. An efficient transcription mechanism is thus essential for the survival and pathogenicity of this bacillus. Although a third of the human population are carriers of this pathogen, only a few contract this disease. This bacillus can lie latent in the host for prolonged periods of time till a mycobacterial infection gets triggered, most often in the setting of decreased host immunity. Studies that help further our understanding of the latent phase of this bacillus are thus vital to understand the mechanisms of pathogenesis and virulence in this organism. This ability of *M. tuberculosis* to survive in the hostile environmental conditions in the carrier is brought about by adaptability to rapidly changing environmental conditions. The survival mechanism is thus crucially dependent on efficient communication between the mechanism that senses the environment and the molecules that regulate transcription.

The DNA dependent RNA polymerase (RNAP) that controls gene expression consists of five domains- two α subunits, one ω subunit and the β and β' domains. The σ -factor reversibly

*Corresponding Author B. Gopal Molecular Biophysics Unit, Indian Institute of Science, Bangalore 560 012 Phone : (+91) 80 2293 3219 Fax: (+91) 80 23600535 Email: bgopal@mbu.iisc.ernet.in

associates with the RNAP and provides the RNAP enzyme with the ability to recognize promoter regions on the DNA template. *M. tuberculosis* has a total of 13 σ -factors: 3 primary σ factors and 10 extra-cytoplasmic function (ECF) σ factors. Differences in the promoter specificity of these σ factors lead to differential gene expression (1,2). The task of environment-dependent transcription modulation is performed by the ECF σ factors. Regulatory mechanisms, in turn, dictate which σ factors get activated to bind to the apo-RNAP and initiate transcription and which ones are not. This regulatory mechanism is coupled to a signal transduction system that senses the environment. The interplay between signal transduction and the transcriptional regulatory mechanisms allows the bacillus to respond to changes in the environment by synthesizing new proteins or down-regulating others.

Studies on the transcription mechanism in *E. coli* have shown that a σ factor directs promoter-specific transcription initiation by specific interactions between two hexamers of a consensus DNA sequence- the Pribnow box (-10 element) and the -35 element. The crystal structure and limited proteolysis experiments on the principal σ factor σ^A revealed a structural arrangement comprising of a series of domains connected by flexible linkers. The utility of this structural arrangement is borne out by the observation that substantial structural rearrangements take place in the σ -factor during transcription initiation. Exposed surfaces of each of these domains were found to be important for RNAP binding (3). Interaction with the core RNAP has been demonstrated to structurally rearrange the σ factor into an active conformation in which the DNA binding regions of σ_2 and σ_4 domains are exposed and appropriately positioned to recognize the -10 and -35 elements (3,4,5,6).

Two distinct types of mechanisms have been proposed to describe the regulation of the activity of the σ factors that belong to the σ^{70} family. Thus while auto-inhibition by the N-terminal domain mediates the activity of the principal σ factor, σ^A , protein-protein interactions mediated by the anti- and anti-anti- σ factors control σ factor concentrations in the case of the ECF σ factors. Other regulatory mechanisms have been proposed wherein σ factor activity is controlled by stimulatory signals (such as the phosphorylation and dephosphorylation processes controlled by the kinases and phosphatases) or mechanisms that can control the intracellular σ factor concentration by localizing it on the inner surface of the cell membrane. In the case of the *E. coli* σ factor σ^E (7) for example, many of the key regulators of σ^E activities (products of the *rse* genes) are co-transcribed with *RpoE* to form an operon : *rpoE*, *rseA*, *rseB* and *rseC*. The protein *RseA* is an anti- σ factor for σ^E whereas the periplasmic *RseB* protein enhances its activity. The activity of σ^E can also be regulated by cytoplasmic factors like guanosine 3',5'-bispyrophosphate (ppGpp). The signaling pathway employed in this process is distinct from the pathway that is activated upon extra-cytoplasmic stress (8). Very little is known of these processes in mycobacteria although recent reports indicate that work to delineate the regulatory mechanism of σ^E and another σ^E -like factor σ^H are presently in progress (9,10,11). The anti- σ factor, as seen in the cases of the *SpoIIAB* (12) and the σ^E -*RseA* complex (4), appears to bind the free σ factor, thereby preventing its interaction with the core RNAP. The σ^{28} /*FlgM* complex (6) on the other hand is different from the others in that *FlgM* can also form a ternary complex with the σ^{28} holoenzyme, thereby destabilizing the σ^{28} /RNAP interaction. The modes of σ factor anti- σ factor interactions also differ between the σ^{70} and σ^{28} families. The anti- σ factor *RseA* is sandwiched between σ^E_2 and σ^E_4 domains of σ^E whereas the *FlgM* protein wraps around the outside of σ^{28} and occludes the core RNAP binding determinants on σ^{28}_2 and σ^{28}_4 .

M. tuberculosis has about 190 transcription regulators (13) which include 13 σ factors, 11 two-component systems, 5 unpaired response regulators, 11 protein kinases and 140 other proteins. The resulting interaction amongst these proteins suggests a complex system of overlapping functions and redundancies (9). Four σ factors, σ^A , σ^B , σ^C and σ^E of the 13 in *M. tuberculosis* are conserved in all the pathogenic mycobacteria. Only four σ factors in *M.*

tuberculosis σ^A , σ^C , σ^D and σ^L have been examined in detail for their roles in virulence and pathogenicity. The ECF σ factor σ^C is essential for lethality in mice but is not required for bacterial survival in this species (14). Based on genomic microarray data, σ^C was demonstrated to modulate the expression of several key virulence associated genes including *hspX*, *senX3* and *mtrA*, a two component sensor kinase and a two component response regulator. The phenotype of the $\Delta \sigma^C$ mutant of *M. tuberculosis* can thus persist in tissues but is attenuated in its ability to elicit lethal immunopathology (14). A recent report also suggests σ^C to be a key regulator of pathogenesis and adaptive survival in the lung and spleen of guinea pigs (15). These *in vivo* studies in two different animal models thus demonstrate the role of σ^C in the pathogenesis and virulence of *M. tuberculosis*. Although σ^C does not appear to have an anti- σ factor located in the same operon, *in silico* analysis for the identification of potential interacting partners for σ^C suggested two proteins SirR and the unannotated protein Rv0093c. However, the interaction between these proteins and σ^C could not be substantiated by experimental evidence.

In this manuscript, we report the biochemical and structural analysis of the domain organization of σ^C . Despite the low sequence similarity between the promoter recognition domains of σ^C with the primary σ -factor σ^A , we observe that the crystal structure of the two promoter recognition domains are conserved. Spectroscopic studies using the intrinsic tryptophan fluorescence as well as surface plasmon resonance experiments suggest that the σ^{C_2} and σ^{C_4} domains interact *in vitro*. Interactions between the two promoter recognition domains of σ^C which involves the occlusion of the Pribnow box recognition region of σ^{C_2} suggests that substantial inter-domain rearrangements would be needed to activate σ^C even in the absence of an anti σ -factor.

Methods

Cloning, Expression and Purification of σ^C , and the σ^{C_2} and σ^{C_4} domains

The details of the expression constructs used in this study are compiled in Table 1. After transforming the plasmid into BL21 (DE3) or Rosetta origami cells (Novagen, Inc.), the cells were grown in Luria broth with an antibiotic selection (ampicillin 100 μ g/ml and chloramphenicol 30 μ g/ml) to an OD₆₀₀ nm of 0.5-0.6. The cells were induced with 0.2 mM IPTG (final concentration). Subsequently, the growth temperature was lowered to 290 K and cells were grown for further 12-18 hrs before they were spun down and stored at 193 K. Full length σ^C (311 amino acids) was purified in denaturing conditions using 8M urea. Refolding of the denatured protein was carried out in a step-wise fashion with five buffer changes (each lasting about 3-4 hours) with decreasing concentration of urea. The recombinant proteins from the other three constructs were purified under native conditions as described earlier (16). The proteins were further purified by size exclusion chromatography using a Superdex S-200 column (Amersham-Pharmacia, Inc.) after the affinity chromatography step. The proteins were concentrated using membrane based centrifugal ultra filtration (Amicon). L-Arginine and L-glutamic acid were added to the final concentration of 50mM each during the concentration step (17). The purity of the samples was analyzed using SDS-PAGE followed by Coomassie blue staining. Both full length σ^C as well as the σ^{C_4} domain have poor solubility and are very unstable. These proteins were freshly purified prior to each biochemical experiment. The molecular weights of the recombinant proteins were also verified by Mass spectrometry on a MALDI-TOF (Bruker Daltonics, Inc) mass spectrometer.

The western blot analysis to determine the molecular weight of σ^C *in situ* was performed according to the standard procedure outlined in Molecular Cloning (18). Cell free lysate of H37Rv was obtained from the TB vaccine testing and research material contract at the Colorado state University. The cell lysate and purified protein samples were resolved in 10% SDS-PAGE, and transferred to a nitrocellulose membrane. A polyclonal antibody raised in rabbit against

$\sigma^{C_{127-311}}$ (a smaller construct containing residues 127-311aa based on the annotated sequence of H37Rv) was used as the primary antibody for σ^C detection. Western blots were developed using the AEC (Sigma-Aldrich, Inc.) substrate with HRP-labeled sheep anti-rabbit IgG (Bangalore Genei Co.)

Site directed mutagenesis experiments were performed using a PCR based method (19). The primers GATAGGCGACGAACCGCGCCACGTCTTGCTGGG (for W164A) and CGATGGCCAGCAACGCAGTTCGGGCGCTGG (for the W203A point variant) were used. These mutations were confirmed by DNA sequencing.

Fluorescence Spectroscopy

All fluorescence studies were performed on a JOBIN YVON FlouoroMax-3 fluorimeter at room temperature. The fluorescence excitation was set at 280 nm and emission spectra were recorded from 300 to 400 nm at a band-width of 1 nm. The excitation and emission slit widths were set to 3 and 5 nm, respectively. Each spectrum is an average of five scans. The spectra were obtained at a protein concentration of $\sim 3 \mu\text{M}$ in 10 mM Tris-HCl, 50 mM NaCl pH 7.5. Interactions between the σ^{C_2} and σ^{C_4} domains were monitored after the two protein samples were mixed and incubated at room temperature for 2 minutes prior to data acquisition.

Surface Plasmon Resonance Experiments

Surface plasmon resonance (SPR) assays were performed on a BIAcore 2000 instrument (BIAcore AB). All experiments were conducted at 25°C. SPR experiments were performed with either the σ^{C_2} and σ^{C_4} domains immobilized onto carboxylated dextran chips (sensor chip CM5 from BIAcore AB) using the standard amine coupling procedure as recommended by the manufacturer. Immobilization resulted in a change in the refractive index corresponding to 700 and 640 resonance units (RU) for σ^{C_2} and σ^{C_4} respectively. Binding and kinetic assays were performed in 50 mM sodium phosphate (pH 7.4), 100 mM NaCl at flow rate of 20 $\mu\text{L}/\text{min}$. The proteins were diluted in this buffer and experiments were carried out at concentrations ranging from 0.8–200 μM . Freshly purified protein samples were used for these binding assays. Dissociation was initiated by replacing the analyte with buffer. The association and dissociation curves were monitored for 120s. Sensograms were analyzed with BIAevaluation software version 2 (BIAcore AB). A 1:1 langmuir binding model was used to fit the curves.

Model building and Refinement of the two domains of σ^C

Crystallization conditions and data collection strategies have been reported previously (16). The data collection and refinement statistics for both the domains are reported in Table 2. The N- and C-terminal domains of *E.coli* σ^E (PDB code 1OR7) were used as starting model(s) for Molecular Replacement (MR). The sequence identity between σ^{C_2} and N-term σ^E is 23% whereas that between the C-term σ^E and σ^{C_4} domain is 45%. MR calculations were performed using the program PHASER(20). The solution for σ^{C_2} and σ^{C_4} had log likelihood gains of 71.52 and 489.97 with corresponding Z-scores of 5.21 and 15.53 respectively. There were two molecules in the asymmetric unit in the case of σ^{C_2} and three in the asymmetric unit for the σ^{C_4} domain. Both structures were refined using tight non-crystallographic symmetry (NCS) restraints. Iterated cycles of model building using Coot (21) and refinement using Refmac (22) led to the final model for σ^{C_2} with an R_{cryst} of 18.9% and R_{free} of 24.3%. The final model σ^{C_4} had R_{cryst} of 21.0 % and R_{free} of 26.7% The final model of σ^{C_2} consists of 88 residues, 4 sulfate ions and 20 water molecules whereas that for the σ^{C_4} domain has 60 residues, 8 sulfate ions and 17 water molecules.

Computational strategies to identify potential σ^C interacting proteins

In *M. tuberculosis* the following σ -anti σ pairs have been reported: σ^D -Rv3413c, σ^E -Rv1222, σ^F -Rv3287c, σ^H -Rv3222c and σ^L -Rv0736 (23,24,25,26,27). σ^D , σ^F , σ^H and their respective anti- σ factors are canonical in the sense that these pairs occur as a part of one operon. σ^C the only member in an operon in both the *M. tuberculosis* strains H37Rv and CDC1551. Assuming that interacting proteins would show correlated expression levels under certain conditions, the correlation coefficients and t values (Student's t test) between a given σ factor and the corresponding anti- σ pair were calculated in different conditions (7H9 medium(N=4), Balb mice(N=4), Scid mice(N=4), stationary state(N=6), Low oxygen dormancy(N=9) using the equations given below:

$$r_{jk} = \left(\sum (x_{ij} - \bar{x}_j)(x_{ik} - \bar{x}_k) \right) / n\sigma_j\sigma_k$$

$$= \left(\sum (x_{ij} - \bar{x}_j)(x_{ik} - \bar{x}_k) \right) / \left(\left(\sum (x_{ij} - \bar{x}_j)^2 \right) \left(\sum (x_{ik} - \bar{x}_k)^2 \right) \right)^{1/2}$$

$$t_{jk} = r_{jk}(N-2)^{1/2} / (1 - r_{jk}^2)^{1/2}$$

To predict all the interacting proteins/anti- σ factor(s) for σ^C , we examined all the transcription regulatory genes that are present in *M. leprae* (*M. leprae* has only 4 σ factors σ^A , σ^B , σ^C , and σ^E). An amino-acid sequence based search was also performed to locate putative anti- σ factors on the basis of the sequence signature (HXXXCXXC) (27). Transmembrane protein prediction was done using the program Conpred (28). These results are compiled in Supplementary Table 1.

Results and Discussion

Characterization of the domain organization of *M. tuberculosis* σ^C

Differences in the annotation of σ^C in the two *M. tuberculosis* strains H37Rv (13) and CDC1551 (29) led to the identification of an N-terminal 126 residue long polypeptide preceding the structured domain σ^C_2 . The σ^C_2 and σ^C_4 domains are connected by a flexible ~25 amino acids long linker. Sequence based prediction of low complexity regions (30) in this protein (Figure 1a) suggests that the N-terminal domain preceding σ^C_2 is largely unfolded. *M. tuberculosis* extra-cytoplasmic σ^C thus appears to be more primary σ factor-like in terms of the domain organization except that it lacks the region 3.2 that lies between the σ^C_2 and σ^C_4 domains and is involved in extended -10 promoter recognition. The sequence based structure alignment of *M. tuberculosis* σ^C is shown in Figure 2 (adapted from reference 2). Interestingly, *Myobacterium leprae* σ^C does not have this N-terminal region. Based on the sequence alignment and patterns of protease sensitivity, four expression constructs of σ^C were examined: the full length σ^C , the smaller construct containing only the σ^C_2 and σ^C_4 domains and the two independent domains σ^C_2 and σ^C_4 (Table 1 and Figure 3). In a western blot experiment using cell free lysate of *M. tuberculosis* H37Rv (obtained from the TB research center, Colorado State University), the polyclonal antibody raised against the shorter length construct (lacking the 126 amino acid polypeptide at the N-terminus) recognized the full-length σ^C . σ^C is thus a 311 amino acids long protein in both the laboratory (H37Rv) as well as the clinical (CDC1551) strains of *M. tuberculosis* (Figure 3).

Structure determination of the σ^C_2 and the σ^C_4 domains

The σ^E_2 and σ^E_4 domains of *E. coli* σ^E were used as search models to solve the structures of *M. tuberculosis* σ^C_2 and σ^C_4 domains by Molecular Replacement. Overall, these two proteins have 32 % identity in the amino acid sequence although the C-terminal region is more conserved than the N-terminal polypeptide. Thus while *M. tuberculosis* σ^C_2 and *E. coli* σ^E_2 have 23 % identity, *M. tuberculosis* σ^C_4 and *E. coli* σ^E_4 are more similar with ~ 44 % sequence

identity. The crystallization of the σ^{C_2} and the σ^{C_4} domains has been reported earlier (16). The data collection and refinement statistics are compiled in Table 2 (more details in Supplementary Figure 1). Despite the low sequence similarity, the overall topology of the σ^{C_2} and the σ^{C_4} domains is similar to that of the known σ factors reported till date (3,4,5,6). The backbone $C\alpha$ superposition between σ^{C_2} with *E. coli* σ^{A_2} shows a root-mean-squared-deviation (rmsd) of 2.97 Å (~8 % identity over 77 amino acid residues) whereas σ^{C_2} superposes better with *E. coli* σ^{E_2} with an rmsd of 1.4 Å (24 % identity over 88 residues). The σ^{C_4} domain which interacts with the -35 promoter element is structurally more conserved with a backbone rmsd of 1.6 Å with the corresponding domain of the primary σ -factor σ^{A_4} . Molecular modeling and docking based on the structure of the *Thermus aquaticus* RNAP suggests that the σ^{C_2} and σ^{C_4} domains would be spatially separated by a distance of ~50 Å (data not shown) when bound to the RNAP. This distance is compatible with the ca 25 residue linker joining the σ^{C_2} and σ^{C_4} domains. Studies on the primary σ -factor σ^A have shown that aromatic and charged residues in region 2 are involved in recognizing the -10 element and subsequent strand separation (31). On the basis of multiple sequence alignment, W203 was found to be universally conserved and is likely to be involved in interactions with the Pribnow box element. Based on a model of *E. coli* σ^E -holoenzyme and the σ^E -RseA structure (4), Campbell *et al* proposed that the *E. coli* anti- σ factor RseA functions by sterically occluding the two primary RNAP-binding regions on σ^E . Activation of the σ^E regulon occurs when σ^E is released from RseA upon degradation by the Hho (DegS) protease. In the σ^E -RseA structure, the anti- σ factor was found to be sandwiched between the σ^{E_2} and the σ^{E_4} domains. Several substitutions in *E. coli* σ^{E_4} , R178G, I181A and V185A were identified as those that led to defective RseA binding (4). In the case of *M. tuberculosis*, the equivalent Arg residue is conserved whereas the other two positions (*E. coli*/*M. tub*) are replaced by (Ile/Leu) and (Val/Ala).

Identification and verification of potential σ^C interacting proteins in *M. tuberculosis*

M. tuberculosis σ^C is different from other ECF σ factors as there is no anti- σ factor located downstream of σ^C in the same operon. To understand the mechanism of regulation of transcription by σ^C , attempts were made to identify the interacting partners that could activate/inactivate this protein. Coimmunoprecipitation using the purified σ^C antibody using the cell free lysate (obtained from the TB research center, Colorado State University) was used to isolate proteins that interact with σ^C . These proteins were identified by *in situ* digestion using trypsin followed by peptide mass-fingerprinting using a MALDI-TOF mass spectrometer and analyzed using MASCOT (Bruker Daltonics, Inc). Few components of RNAP could be detected at high confidence levels (data not shown). However, no potential anti- σ factor could be identified in this experiment. Several computational tools were also used to identify proteins that could potentially interact with σ^C . These results including relevant entries from the database STRING (32) are compiled in Table 3. The application of this tool for the prediction of protein-protein interactions suffers from the problem that functional interaction does not necessarily imply direct physical interaction. Based on the co-occurrence of genes in related species, proteins exhibiting similar phylogenetic profiles can be predicted to be functionally linked i.e. they occur as a structural complex or are involved in a common metabolic pathway. Although 29 potential interacting proteins could be identified using this approach, none showed a significant correlation in their mRNA expression levels with that of σ^C . The Rosetta tool for gene fusion analysis (33) led to the identification of the gene Rv0093c. In this method the existence of a fusion protein in one genome allows the prediction of the interaction between the single domain proteins in other genomes. Rv0093c also has an amino-acid sequence signature proposed for anti- σ factors that regulate oxidative stress (27) and a conditional correlation was observed between the expression level of this protein versus σ^C in one DNA microarray data-set. A pertinent observation in this regard is that notwithstanding the large errors involved in the gene expression levels obtained using DNA microarray technology, well

characterized σ -anti σ pairs exhibit significant correlation ($\alpha=0.05$) under specific environmental or growth conditions (Table 3b).

A sequence based search for RseA-like proteins in the *M. tuberculosis* genome led to the identification of a protein SirR (32 % identity between the *E. coli* RseA sequence that interacts with σ^E and *M. tuberculosis* SirR). The annotation of SirR in the *M. tuberculosis* genome describes it as an Iron dependent transcription repressor. Two strategies, one involving co-expression using pET-Duet1 vector and the other by *in vitro* studies using purified recombinant proteins were adopted to examine interactions between σ^C and the predicted anti- σ factors SirR and Rv0093c. In the co-expression approach, σ^C was cloned with a poly-histidine tag at the N-terminus to enable the complex to be purified by affinity chromatography. No interaction could be detected between either of these proteins and σ^C *in vitro* (data not shown). This finding could probably be rationalized on the basis of the variations seen in residues that are involved in RseA recognition.

Interaction between the two promoter recognition domains σ^C_2 and σ^C_4

Fluorescence measurements using the intrinsic tryptophan residue in σ^C_2 were used to monitor the interactions between the two promoter recognizing domains of σ^C . The fluorescence spectra are shown in Figure 4. There are two tryptophans in σ^C_2 (region 2) and none in σ^C_4 (region 4) (Figure 4b). This fortuitous distribution of tryptophan residues helped us examine the interactions between the σ^C_2 and σ^C_4 domains. A fluorescence spectrum of native σ^C (127-311 residues) showed an emission maximum at 342 nm while σ^C_2 showed an emission maximum at 349 nm. Upon the addition of σ^C_4 in stoichiometric ratio, a blue shift (~ 7 nm) in the fluorescence spectrum was observed with a reduction in the emission intensity. A representative binding reaction wherein the σ^C_4 domain is titrated into the σ^C_2 domain is shown in Figure 4a. This fluorescence titration suggests a weak interaction between the σ^C_4 and σ^C_2 domains ($K_d \sim 2 \mu\text{M}$).

Of the two tryptophans in σ^C_2 , Trp-203 is involved in DNA melting (Pribnow Box element). Based on molecular modeling analysis (data not shown) Trp-164 is likely to interact with the RNAP. These observations led us to investigate the specificity of interactions (given the fact that the two domains are connected by a flexible linker of ca 25 amino acids long) and identify the region where σ^C_4 binds σ^C_2 . To address these questions, two point variants of σ^C viz W164A and W203A were constructed in $\sigma^C_{127-311}$ (medium length σ^C that lacks the positively charged N terminal domain which contains three tryptophan residues). The W164A mutant protein had a fluorescence emission maximum at 335 nm whereas the W203A variant had its emission maximum at 353 nm (Figure 4b). The blue shift seen in the W164A variant suggests that σ^C_4 interacts σ^C_2 in the region that would lead to the partial burial of W203 (Figure 4c). Interactions between the σ^C_2 and σ^C_4 domains thus result in the occlusion of the Pribnow box recognition element.

The interaction between the σ^C_2 and σ^C_4 domains was also monitored by Surface Plasmon Resonance experiments (Figure 4d). SPR studies of the interaction between the σ^C_2 and σ^C_4 domains suggest a low affinity binding between these two domains ($K_d=1.81\pm0.03\mu\text{M}$). The binding affinity and kinetic parameters were comparable when either the σ^C_2 and σ^C_4 domain was immobilized. The highly polar nature of this interdomain interaction was apparent from a size exclusion chromatography experiment performed at medium salt concentrations (250mM NaCl) where the two domains migrate separately. This was also supported by fluorescence quenching experiments where increasing salt concentrations not only reduced the fluorescence quenching but also resulted in a red shift in the emission maximum (Supplementary Figure 3).

In summary, the structural and biophysical studies on the two promoter recognition domains of σ^C shows an interaction between the σ^C_2 and σ^C_4 domains that is mostly governed by polar

residues. This interaction involves the occlusion of the region of σ^C that participates in the recognition of the -10 promoter element. The binding of *M. tuberculosis* σ^C to the core RNAP would thus involve substantial structural re-arrangement to release σ^C from its auto-inhibited state. These observations thus provide an alternate mechanism for the regulation of the ECF σ -factor, σ^C .

Supplementary Material

Refer to Web version on PubMed Central for supplementary material.

References

1. Helmann JD. *Advances in Microbial Physiol* 2002;46:47–109.
2. Waagmeester A, Thompson J, Reyrat JM. *Trends Microbiol* 2005;13:505–509. [PubMed: 16140533]
3. Campbell EA, Muzzin O, Chlenov M, Sun JL, Olson CA, Weinman O, Trester-Zedlitz ML, Darst SA. *Mol Cell* 2002;9:527–39. [PubMed: 11931761]
4. Campbell EA, Tupy JL, Gruber TM, Wang S, Sharp MM, Gross CA, Darst SA. *Mol. Cell* 2003;11:1067–1078. [PubMed: 12718891]
5. Murakami K, Darst SA. *Curr. Opin. struct. Biol* 2003;13:131–139.
6. Sorenson MK, Ray SS, Darst SA. *Mol. Cell* 2004;14:127–138. [PubMed: 15068809]
7. Lonetto M, Gribskov M, Gross CA. *J. Bacteriol* 1992;174:3843–3849.
8. Costanzo A, Ades SE. *J. Bacteriol* 2006;188:4627–4634. [PubMed: 16788171]
9. Manganelli R, Dubnau E, Tyagi S, Kramer FR, Smith I. *Mol. Microbiol* 1999;31:715–724. [PubMed: 10027986]
10. Manganelli R, Voskuil MI, Schoolnik GK, Dubnau E, Gomez M, Smith I. *Mol. Microbiol* 2002;45:365–374. [PubMed: 12123450]
11. Manganelli R, Proveddi R, Rodrigue S, Beaucher J, Gaudreau L, Smith I. *J. Bact* 2004;186:895–902. [PubMed: 14761983]
12. Campbell EA, Masuda S, Sun JL, Muzzin O, Olson CA, Wang S, Darst SA. *Cell* 2002;108:795–807. [PubMed: 11955433]
13. Camus JC, Pryor MJ, Medigue C, Cole ST. *Microbiology* 2002;148:2967–2973. [PubMed: 12368430]
14. Sun R, Converse PJ, Ko C, Tyagi S, Morrison NE, Bishai WR. *Mol. Microbiol* 2004;52:25–38. [PubMed: 15049808]
15. Karls RK, Guarner J, McMurray DN, Birkness KA, Quinn FD. *Microbiology* 2006;152:1591–1600. [PubMed: 16735723]
16. Costanzo DA, Ades SE. *J. Bacteriol* 2006;188:4627–4634. [PubMed: 16788171]
17. Thakur KG, Gopal B. *Acta Cryst* 2005;F61:779–781.
18. Golovanov AP, Hautbergue GM, Wilson SA, Lian LY. *J. Am. Chem. Soc* 2004;126:8933–8939. [PubMed: 15264823]
19. Sambrook, J.; Russell, DW. *Molecular Cloning: A laboratory manual*. Third edition. Cold Spring Harbour Press; 2001.
20. Shenoy AR, Viswesvariah SS. *Anal. Biochem* 2003;319:335–336. [PubMed: 12871732]
21. Storoni LC, McCoy AJ, Read RJ. *Acta Cryst* 2004;D60:432–438.
22. Emsley P, Cowtan K. *Acta Cryst* 2004;D60:2126–2132.
23. Murshudov GN, Vagin AA, Dodson EJ. *Acta Cryst* 1997;D53:240–255.
24. Raman S, Hazra R, Dascher CC, Husson RN. *J. Bacteriol* 2004;186:6605–6616. [PubMed: 15375142]
25. Manganelli R, Voskuil MI, Schoolnik GK, Smith I. *Mol. Microbiol* 2001;41:423–437. [PubMed: 11489128]
26. Beaucher J, Rodrigue S, Jacques P-E, Smith I, Brzezinski R, Gaudreau L. *Mol Microbiol* 2002;45:1527–1540. [PubMed: 12354223]
27. Song T, Dove SL, Lee KH, Husson RN. *Mol. Microbiol* 2003;50:949–959. [PubMed: 14617153]
28. Hahn MY, Raman S, Ananya M, Husson RN. *J. Bacteriol* 2005;187:7062–7071. [PubMed: 16199577]

28. Arai M, Mitsuke H, Ikeda M, Xia J-X, Kikuchi T, Satake M, Shimizu T. *Nuc Acids Res* 2004;32:W390–W393.
29. Fleischmann RD, Alland D, Eisen JA, Carpenter L, White O, Peterson J, DeBoy R, Dodson R, Gwinn M, Haft D, Hickey E, Kolonay JF, Nelson WC, Umayam LA, Ermolaeva M, Salzberg SL, Delcher A, Utterback T, Weidman J, Khouri H, Gill J, Mikula A, Bishai W, Jacobs WR Jr, Venter JC, Fraser CM. *J Bacteriol* 2002;184:5479–90. [PubMed: 12218036]Jr
30. Priluski J, Felder CE, Zeev-Ben-Mordehai T, Rydberg EH, Man O, Beckmann JS, Silman I, Sussman JL. *Bioinformatics* 2005;21:3435–3438. [PubMed: 15955783]
31. Tomsic M, Tsujikawa L, Panaghie G, Wang Y, Azok J, deHaseth PL. *J. Biol. Chem* 2001;276:31891–31896. [PubMed: 11443133]
32. Von Mering C, Jensen LJ, Snel B, Hooper SD, Krupp M, Foglierini M, Jouffre N, Huynen MA, Bork P. *Nuc. Acid. Res* 2005;33:D433–D437.
33. Strong M, Graeber TG, Beeby M, Pellegrini M, Thomson MJ, Yeates TO, Eisenberg D. *Nuc. Acid. Res* 2003;31:7099–7109.

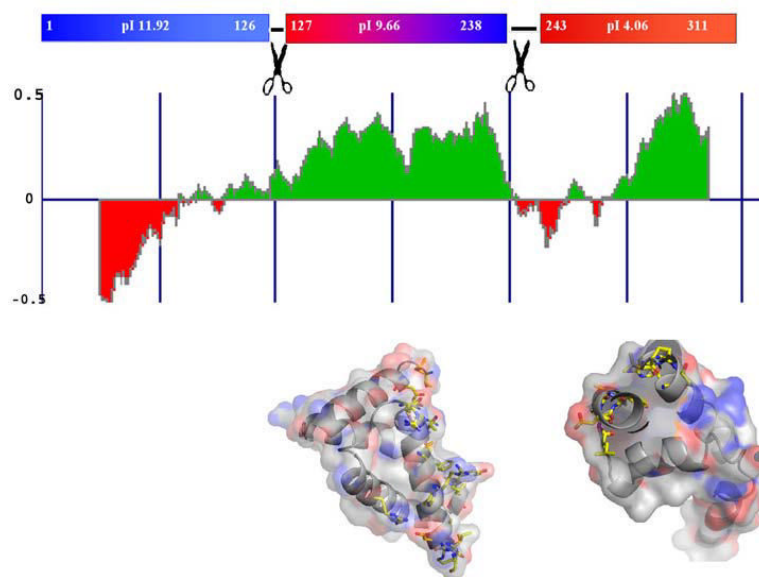
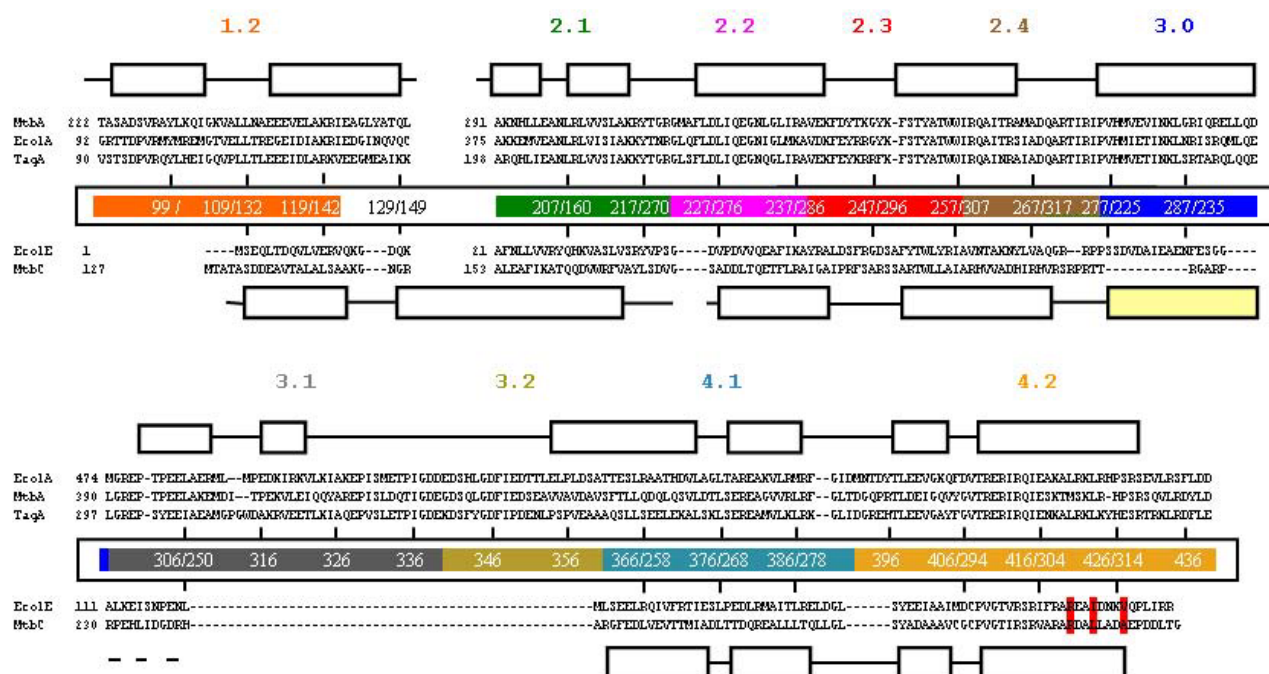


Figure 1.

Domain Organization of *M. tuberculosis* σ^C . (A) Estimate of the folded nature of the three domains of σ^C calculated using the program FoldIndex (30). These estimates are consistent with presently available biochemical data on the principal σ factor σ^A . The top panel shows the pI of different domains in σ^C . (B) Molecular surface representation of the two domains of σ^C . Residues that interact with the -10 promoter element (σ^C_2) and the -35 element (σ^C_2) are highlighted in a ball-and-stick representation. These two domains are connected by a flexible linker.

**Figure 2.**

Structure based sequence alignment of σ^{70} families of σ factors. The top three sequences correspond to those of the principal σ factors with the secondary elements that correspond to the *T. aquaticus* σ^A (3). The two sequences below those of the principal σ factors correspond to ECF σ factors. The secondary structure representation in this case is based on *M. tuberculosis* σ^C . Regions of the σ factor that have been implicated in promoter recognition are highlighted. The residues crucial for the interactions with RseA in case of *E. coli* σ^E are shown in red. The abbreviations are: MtbC: *M. tuberculosis* σ^C , MtbA: *M. tuberculosis* σ^A , EcolA: *E. coli* σ^A , EcolE: *E. coli* σ^E , TaqA: *T. aquaticus* σ^A .

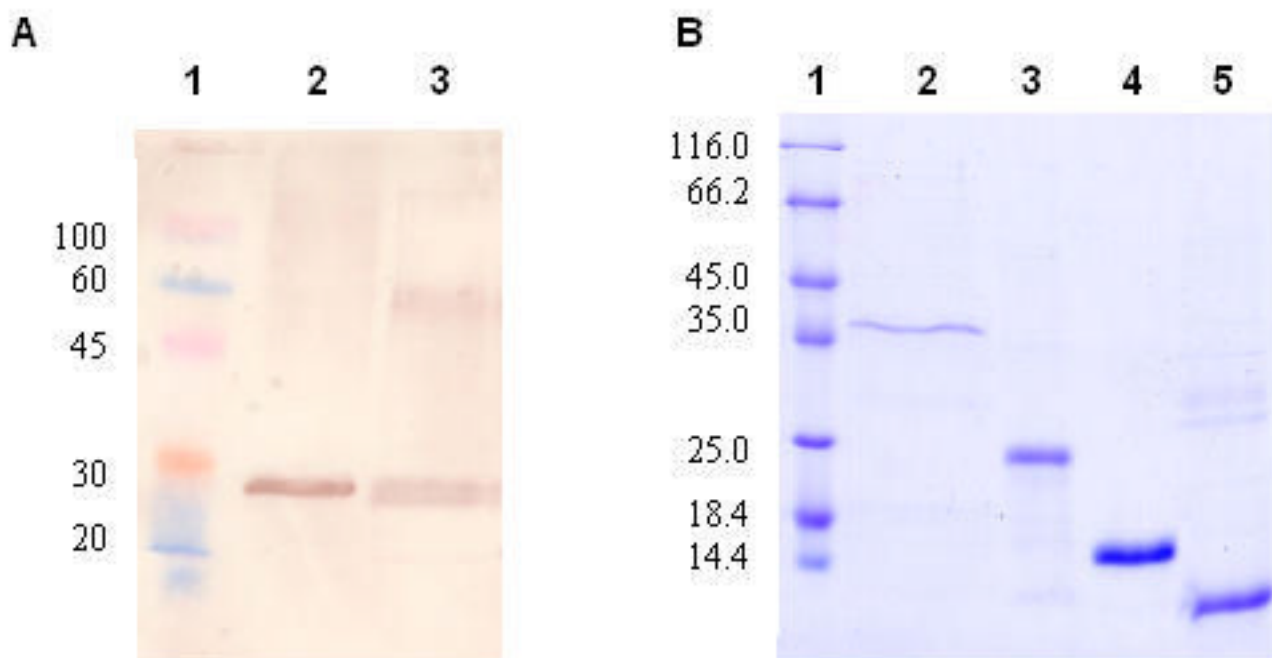
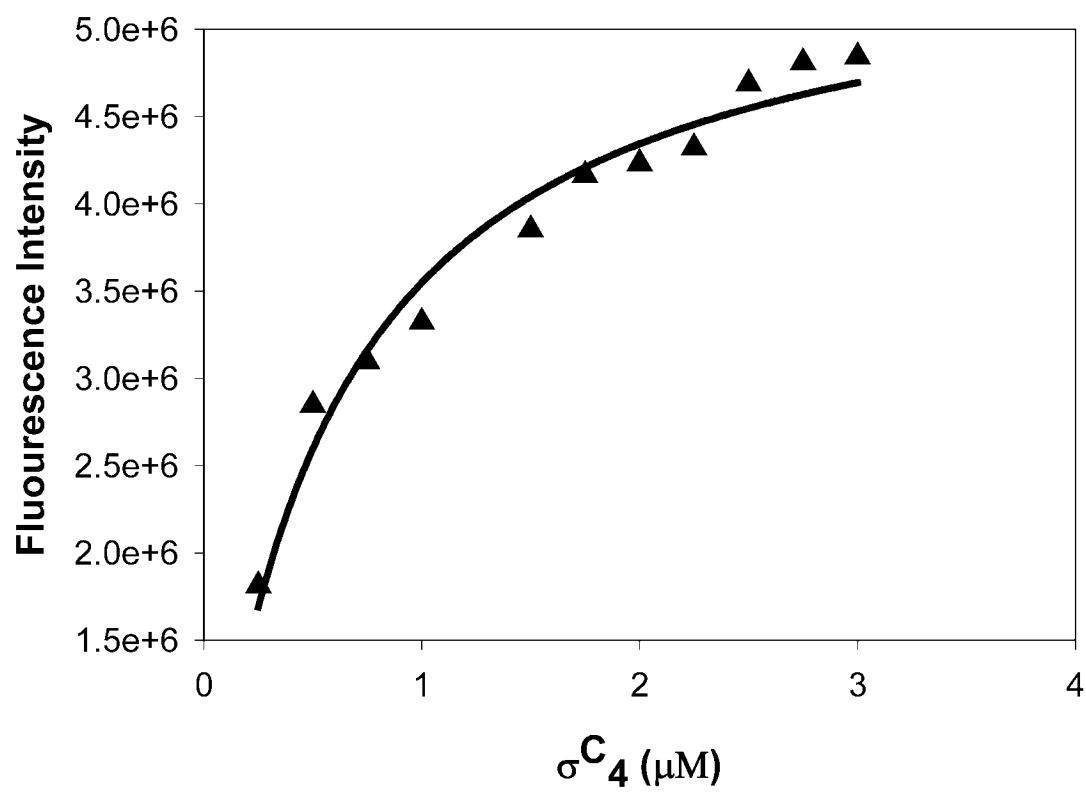
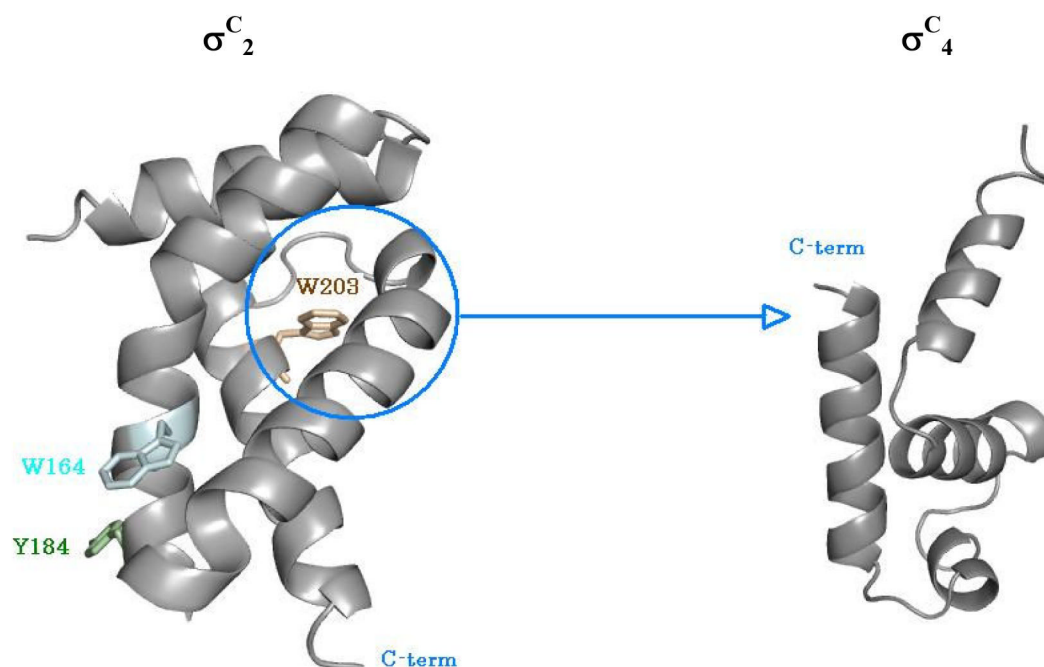
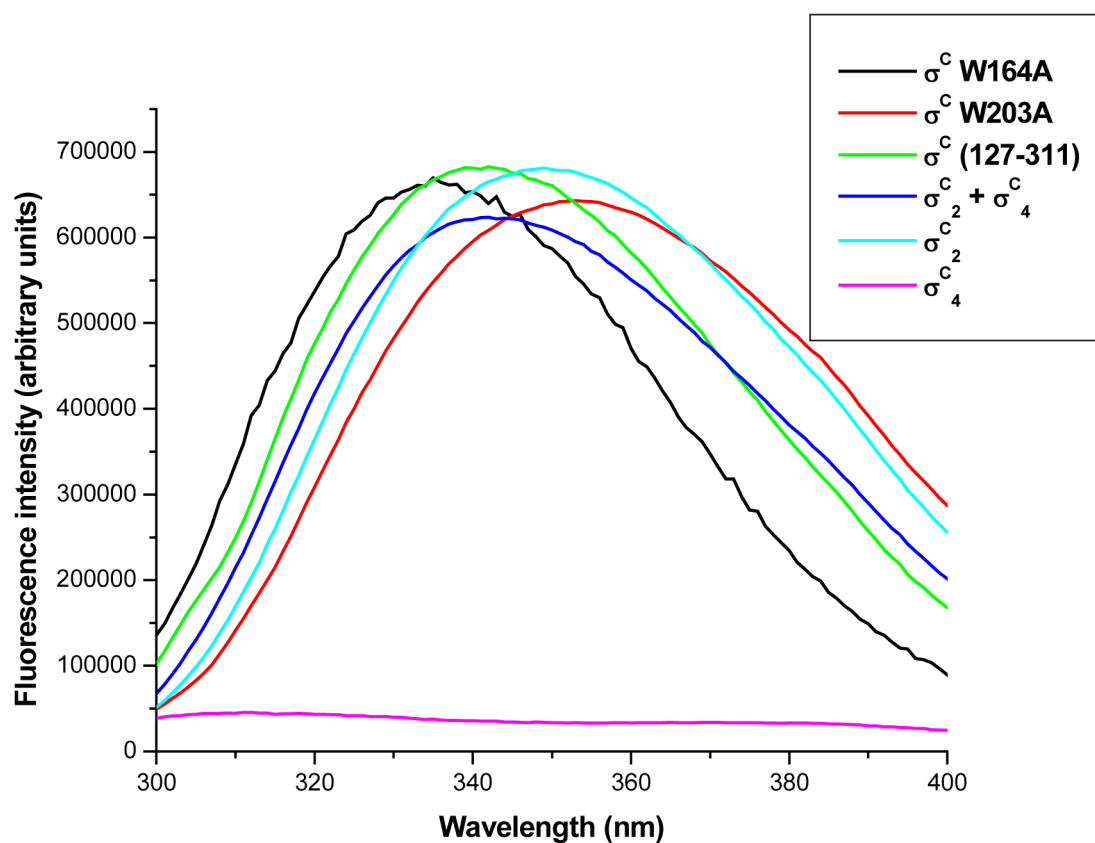


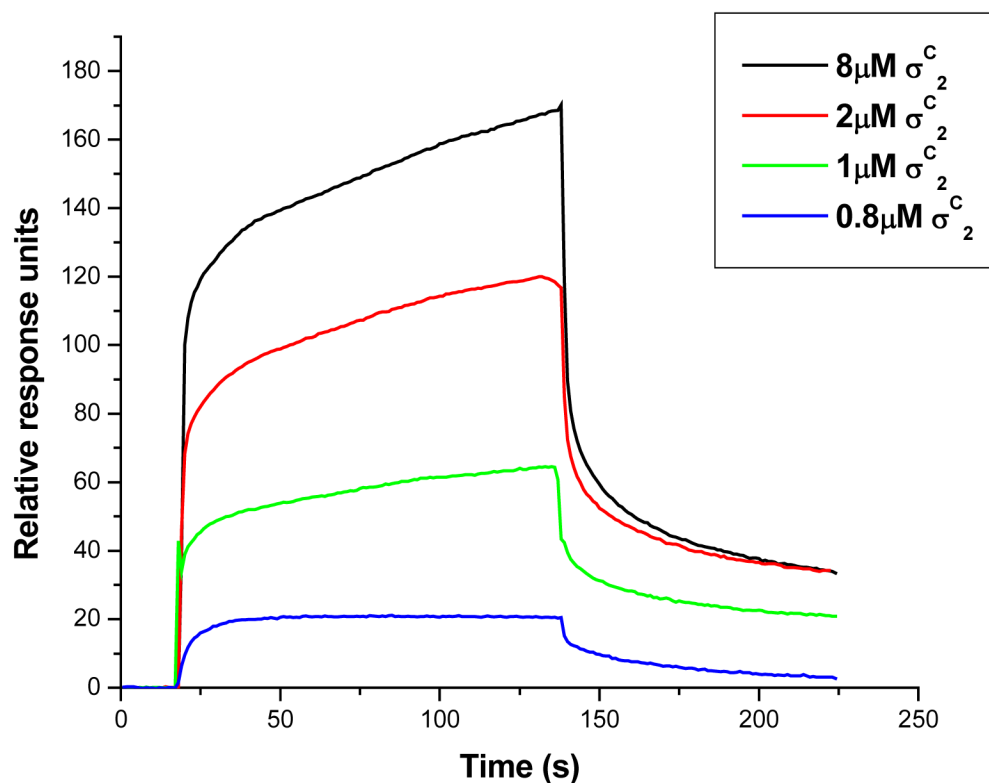
Figure 3.

***M. tuberculosis* σ^C has an N-terminal polypeptide preceding the σ^{C_2} and σ^{C_4} domains.**

(A) Western blot analysis using the cell free lysate of *M. tuberculosis* H37Rv. The size of the protein corresponds to that of the full-length 311 residue protein of σ^C . Lane 1: prestained protein marker, lane 2: *M. tuberculosis* H37RV cell free lysate, lane 3: purified $\sigma^{C_{1-311aa}}$ (B) 12% SDS PAGE gel showing different constructs used in the present study. Lane 1: protein marker, lane 2: $\sigma^{C_{1-311aa}}$ (35.3KDa), lane 3: $\sigma^{C_{127-311aa}}$ (22.5KDa), lane 4: σ^{C_2} (14.7KDa), lane 5: σ^{C_4} (9.5KDa). The details of these expression constructs are given in Table 1.





**Figure 4.**

The σ^{C_2} and σ^{C_4} domains of σ^C interact with each other in the absence of core RNA polymerase. **A.** Interaction between the σ^{C_2} and σ^{C_4} domains monitored by the Fluorescence spectroscopy. In this experiment the quenching of the intrinsic tryptophan fluorescence was monitored as a titration with increasing concentrations of the σ^{C_4} domain (that has no tryptophan residues). This data was analyzed using the SigmaPlot software suite (Systat, Inc.). **B.** Changes in the intrinsic tryptophan fluorescence suggests an interaction between the σ^{C_2} and σ^{C_4} domains. **C.** Spatial orientations of the two tryptophan and one tyrosine residues on σ^{C_2} . The probable site for interaction is shown with the circle. **D.** A representative SPR sensogram that shows interactions between the σ^{C_2} and σ^{C_4} domains. In this experiment, σ^{C_4} was immobilized on the CM-5 chip (Amersham-Pharmacia, Inc.) while the σ^{C_2} domain was used as the analyte. The experiments were performed with different concentrations of σ^{C_2} .

Table 1List of Expression constructs used in the analysis of the domain organization of *M. tuberculosis* σ^C

S.No	Construct	Restriction sites used 5', 3'	Construct size
1	pET15b- $\sigma^C_{127-311aa}$	NdeI, BamHI	127-311aa
2	pET15b- σ^C_2	NheI, XhoI	127-238aa
3	pET15b- σ^C_4	NdeI, BamHI	243-311aa
5	pETduet1- σ^C	EcoRI, HindIII	1-311aa
6	pETduet- σ^C - <i>Rv0093c</i>	EcoRI, HindIII; NdeI-XhoI	127-311; 1-95
7	pETduet- σ^C - <i>SirR</i>	EcoRI, HindIII; NdeI-KpnI	127-311; 88-149

Table 2

Summary of data collection, processing and refinement statistics

	σ^C_2	σ^C_4
Wavelength (Å)	1.54	1.54
Resolution (Å)	35.01-2.70 (2.89-2.70)	40.29-3.0 (3.16-3.0)
Number of reflections	45969 (6060)	23915 (2920)
Number of unique reflections	17709 (2612)	7040 (1002)
Completeness	99.8 (99.2)	99.4 (97.9)
Redundancy	2.6 (2.3)	3.4 (2.9)
R _{sym}	0.087 (0.387)	0.105 (0.546)
I/ σ	10.9 (2.3)	11.1 (2.0)
R _{cryst}	20.1 (26.0)	20.8 (33.8)
R _{free}	24.7 (24.7)	26.4 (33.2)

^a Values for outer shells are given in paranthesis.^b $R_{sym} = \sum_j |<I> - I_j| / \sum <I>$ where I_j is the intensity of the j^{th} reflection and $<I>$ is the average intensity.^c $R_{cryst} = \sum_{hkl} |F_o - F_c| / \sum_{hkl} |F_o|$ ^d R_{free} was calculated as for R_{cryst} but on 5 % of the data excluded from the refinement calculation.

Table 3

Computational analysis of proteins that can interact with σ^C . (A) Results compiled from the program STRING (32) and (B). Analysis of co-expression levels of known σ / anti σ pairs in *M. tuberculosis*.

(A)		Gene	Neighborhood	Gene fusion	Co-occurrence	Text mining	Homology	Score
	name							
	SigM	-	-	-	+	+	-	0.726
	Rv0093c	-	-	+	-	-	-	0.693
	RpoE	-	-	-	+	+	+	0.390
	SigE	-	-	-	+	+	+	0.352
	Upk	-	-	-	+	+	-	0.267
	LepA	+	+	-	-	-	-	0.256
	DapF	-	-	-	+	-	-	0.226
	Rv3676	-	-	-	+	-	-	0.223
	SigG	-	-	-	+	-	+	0.222
	Rv1318c	-	-	-	+	-	-	0.222
(B)		Stationary	Low oxygen	7h9	Balb	Scid		
Name								
Rv3416(whiB3)	-0.69 (-1.9)	0.64 (1.7)	-0.96 (-6.9)	-0.87 (-3.9)	0.89 (3.9)			
Rv3413(anti- σ^D)	0.92 (4.7)	-0.67(-1.8)	0.55 (1.3)	-0.38 (-0.8)	-0.34 (-0.7)			
Rv3287(anti- σ^F)	0.50 (1.2)	0.41 (0.9)	0.99 (14.0)	-0.63 (-1.6)	-0.66 (-1.8)			
Rv3229(anti- σ^H)	0.28 (0.6)	0.99 (14.0)	0.43 (1.0)	0.34 (0.7)	-0.28 (-0.6)			
Rv0736(anti- σ^I)	0.98 (9.8)	0.96 (8.9)	-0.98 (-1.8)	-0.67 (-1.8)	0.96 (6.9)			
Rv0093c	-0.76 (-2.3)	-0.81 (-2.8)	0.92 (4.7)	-0.42 (-0.9)	-0.64 (-1.6)			

Legend: Expression levels are correlated under different conditions. Stationary: stationary phase of growth; Low oxygen: anaerobic conditions; 7h9: growth in 7H9 medium; Balb: *M. tuberculosis* isolated from immune competent Balb/c mice; scid: *M. tuberculosis* isolated from severe combined immune-deficient (SCID) mice.